Lecture #6
In Vivo Water

- Topics
  - Hydration layers
  - Tissue relaxation times
  - Magic angle effects
  - Magnetization Transfer Contrast (MTC)
  - CEST
- Handouts and Reading assignments
  - Mathur-De Vre, R., "The NMR studies of water in biological systems", Prog. Biophys. Molec. Biol. Vo1 35, pp 101-134, 1979.
  - Bydder, M., et al., "The magic angle effect: a source of artifacts, determinant of image contrast, and technique for imaging", JMRI,25:290-300, 2007.
  - Henkelman, RM, et al., "Magnetization transfer in MRI: a review", NMR in Biomedicine, 14:57-64, 2001.
  - van Zijl, P., et al., "Chemical exchange saturation transfer (CEST): What is in a name and what isn't", MRM 65:927-948, 2011.

Relaxation Recap

- NMR relaxation is due to interactions between nuclear spins and local fluctuating fields arising from…
  - Thermal motion of the lattice
  - Molecular motion
  - Chemical exchange processes
  - Paramagnetic centers
- Effects of these interactions depend on the time scale and nature of the motion.
  - T_1 most sensitive to fluctuations at the Larmor frequency $\omega = \gamma B_0$.
  - T_2 sensitive to fluctuations at the very low frequency $(\omega = 0)$.
  - $T_{1\rho}$ most sensitive to fluctuations at the Rf frequency $\omega = \gamma B_1$.

Note, we haven't yet discussed $T_{1\rho}$ or paramagnetic effects.

In Vivo Water

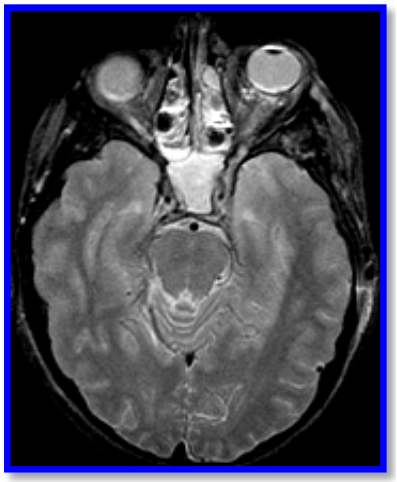

- Relaxation times of in vivo water protons are typically much shorter and diffusion constants much lower than those of pure water.
- A significant fraction of in vivo water is associated with macromolecules in the form of an hydration layer.
- Hydrogen bonding to hydrophylic surfaces results in restricted motion, cross-relaxation, and chemical exchange effects.

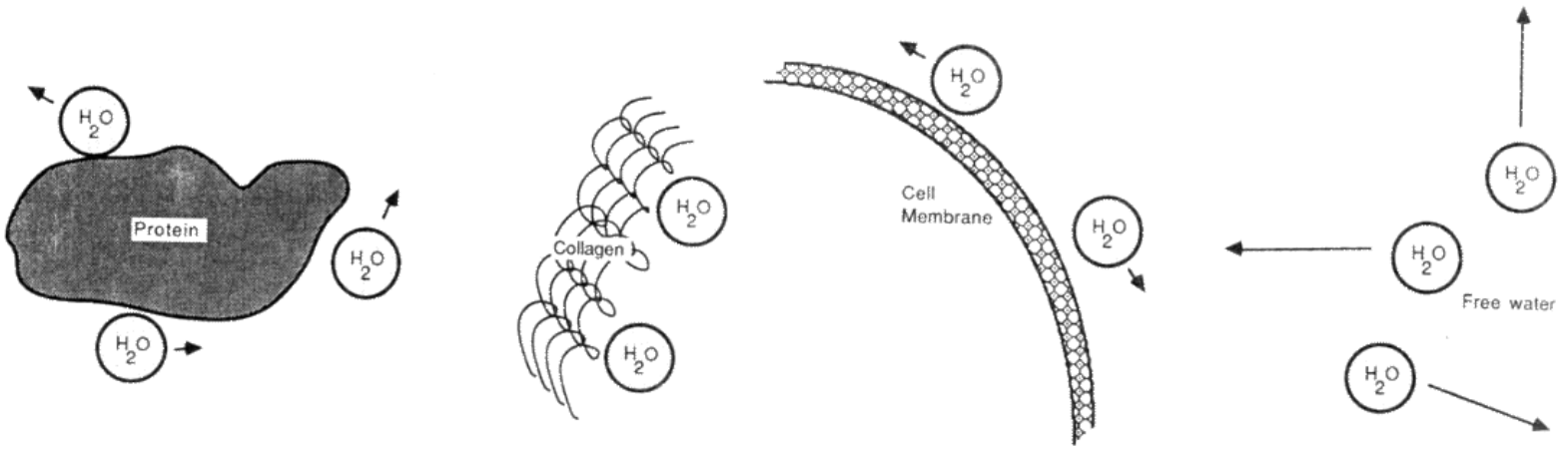

Edelman, et al., *Clinical MRI*, W.B. Saunders Co, Phil., 1996.

Tissue Water Models

- A two compartment model for biological water:

  Free water relaxation rates: $1/T_{1f}$, $1/T_{2f}$

  Hydration water relaxation rates: $1/T_{1r}$, $1/T_{2r}$

  Exchange relaxation rate: $1/\tau_{ex}$

  Water fractions: f_f and f_r

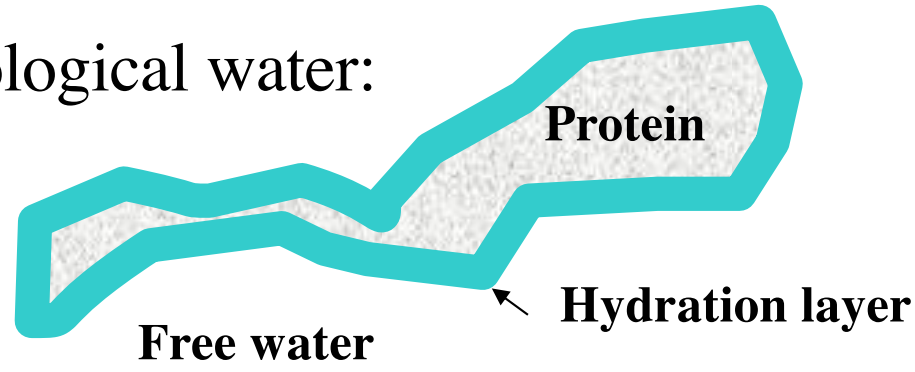

- The two water pools are in fast exchange leading to relaxation rates being avearges of the rates for the two pools.

$$\frac{1}{T_1} = \frac{f_f}{T_{1f}} + \frac{f_r}{T_{1r}}$$

(f_f: free water fraction; f_r: restricted water fraction)

$$\frac{1}{T_2} = \frac{f_f}{T_{2f}} + \frac{f_r}{T_{2r}}$$

- There are also three compartment models which add a tightly bound water "ice-like" pool. This lead to:
  - Tissue T_1 dominated by total water content and fraction in the hydration layer
  - Tissue T_2 dominated by thickness of hydration layer as well as the size of tightly bound pool (see Fullerton, et al, Mag Res Imag, 1:209-226, 1982).

Measuring T_1 and T_2

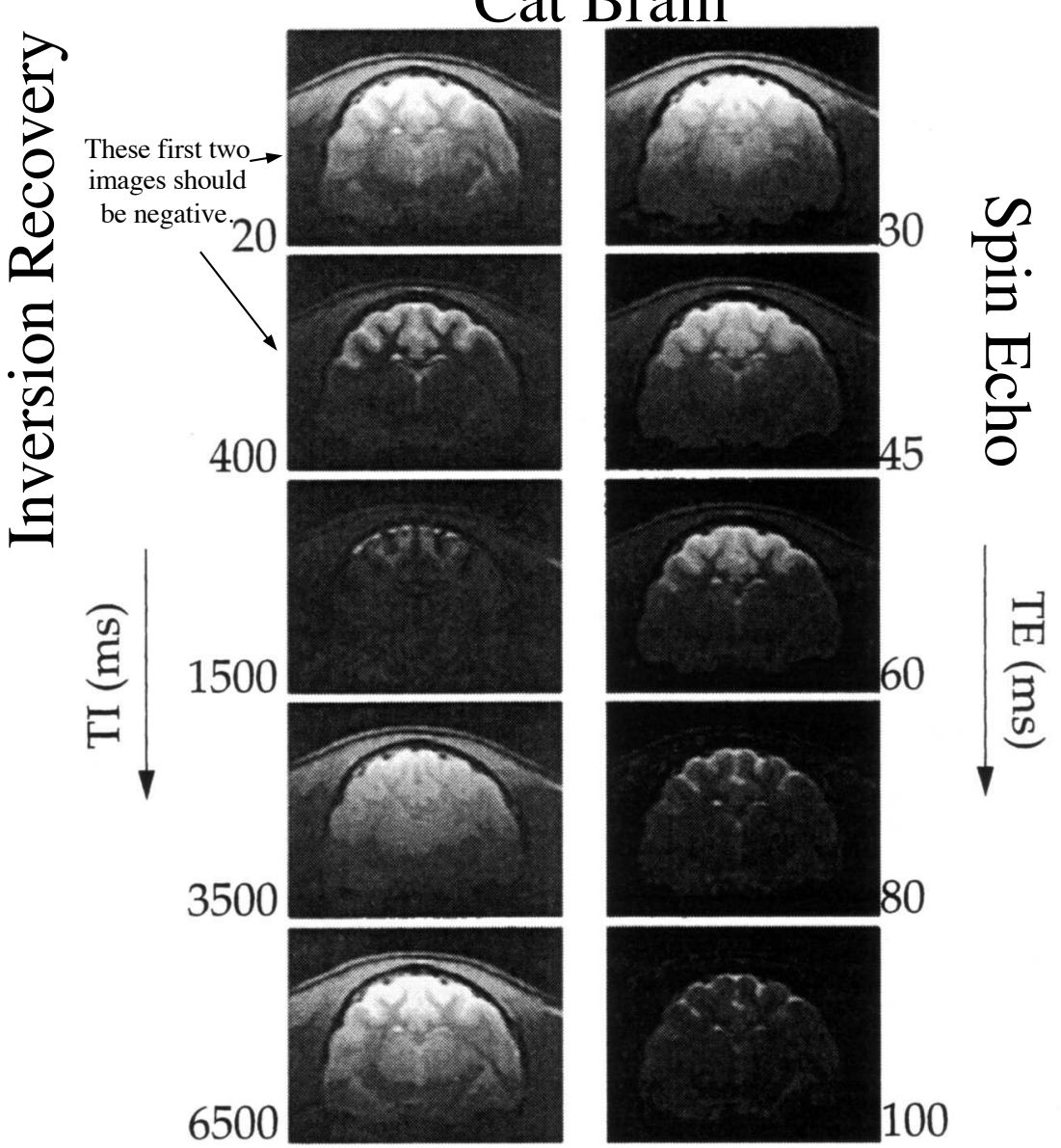

Computed Images

T_1 T_2

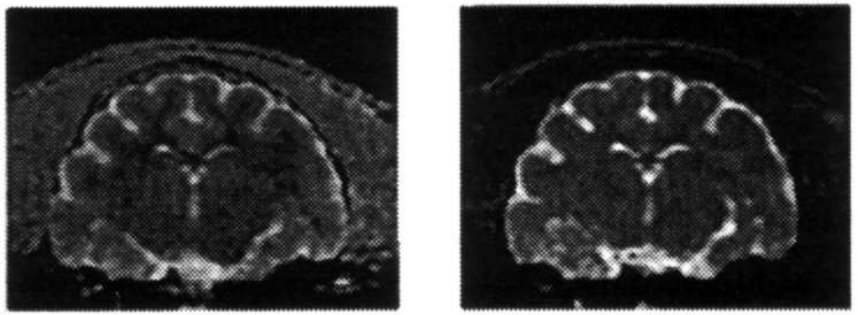

de Graaf, *In Vivo NMR Spectroscopy*, Wiley, 2002.

Biological Water T_1s and T_2s

1.5T

"proton density"
short TE
long TR

"T_1-weighted"
short TE
short TR

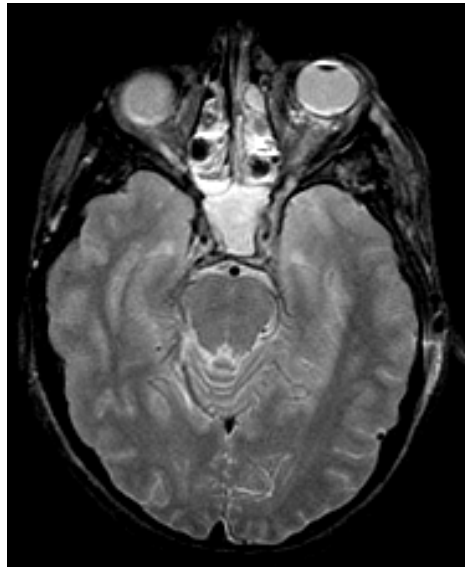

"T_2-weighted"
long TE
long TR

1.5T	T_1	T_2	
White matter	760	90	(ms)
Gray matter	1090	100	
CSF	3000	1500	
Muscle	950	40	
Fat	200	50	
Blood	1200	220	

Biological Water T_1s and T_2s

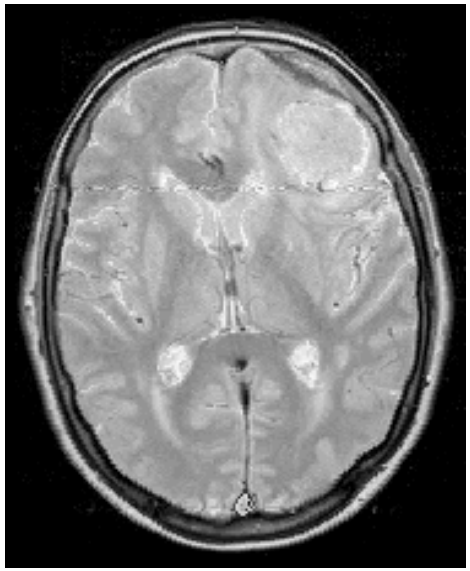

"proton density"

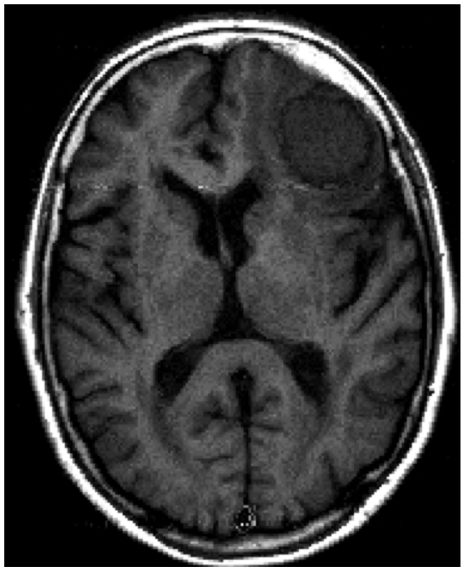

"T_1-weighted"

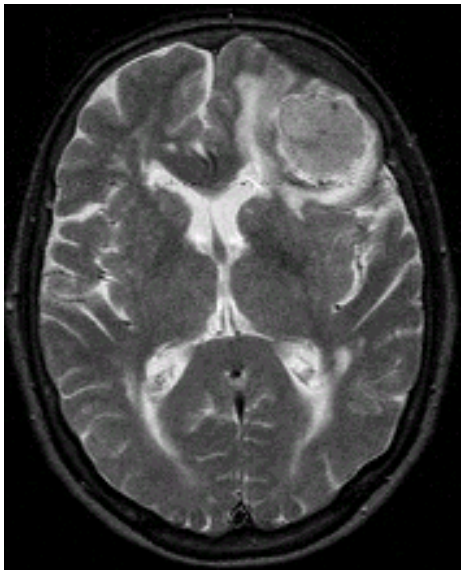

"T_2-weighted"

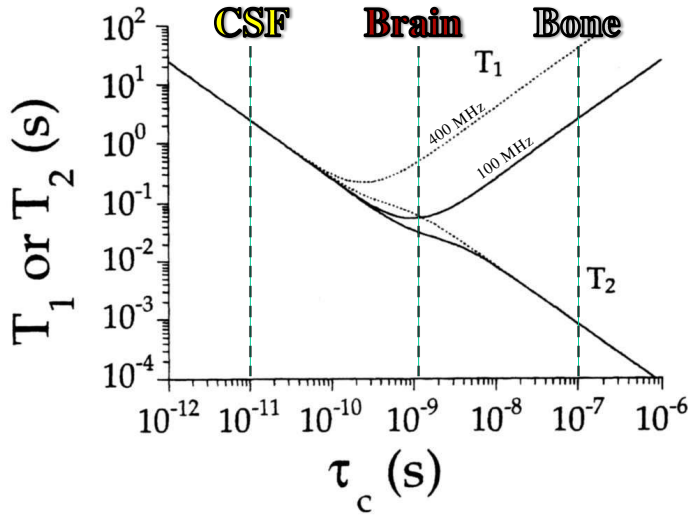

What do these images tell us about the tissue in this tumor versus normal brain?

Biological Water T_1s and T_2s

Table 2.6. Longitudinal and transverse relaxation times of water in biological tissues at different magnetic field strengths[1]

	Magnetic field strength			
	1.5 T		4.0 T	
Human	T_1 (ms)	T_2 (ms)	T_1 (ms)	T_2 (ms)
Brain, gray matter	1099	94	1348	70
white matter	741	77	904	55
Muscle	1140	30	1830	26
	Magnetic field strength			
	2.0–2.5 T		4.7 T	
Rat	T_1 (ms)	T_2 (ms)	T_1 (ms)	T_2 (ms)
Brain	1325	69	1995	67

[1]Reported values are average relaxation times from reported literature [241–256].

de Graaf, *In Vivo NMR Spectroscopy*, Wiley, 2002.

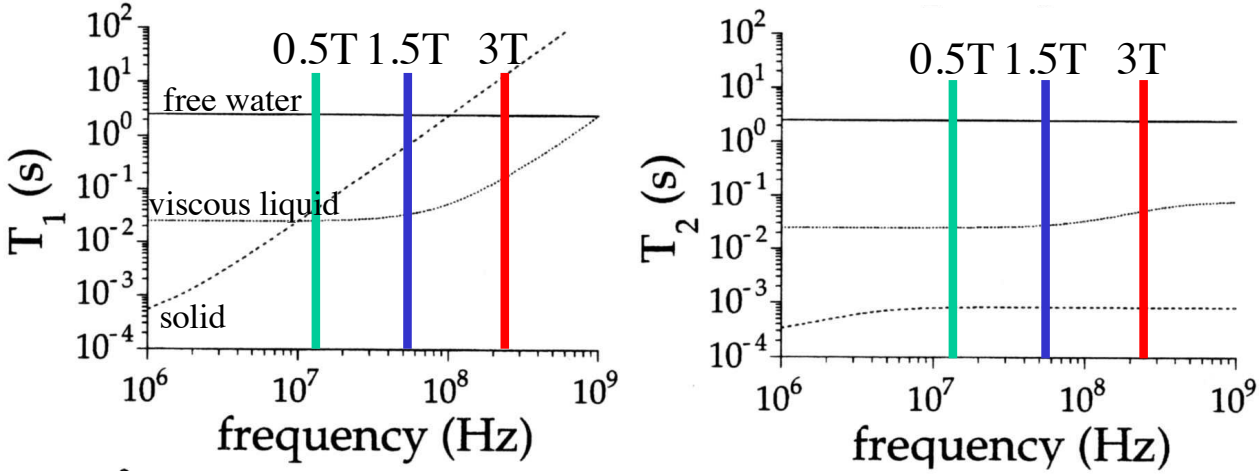

^{1}H Brain Metabolite T_1s and T_2s

Table 2.7. Longitudinal and transverse relaxation times of ^{1}H containing brain metabolites at different magnetic field strengths[1]

		Magnetic field strength				
		1.5 T[2]	2.0–2.35 T[2]	4.0 T[2]	4.7 T[3]	7.0 T[3]
T_1 (ms)	NAA	1485	1505	1386	1970	1890
	tCr	1543	1384	1545	1780	1590
	Cho	1407	1117	1158	1370	1410
T_2 (ms)	NAA	349	372	223	250	168
	tCr	209	242	140	180	132
	Cho	348	346	168	220	209

[1]Reported values are average relaxation times from reported literature [257–272].
[2]Measured on humans.
[3]Measured on rats.

de Graaf, *In Vivo NMR Spectroscopy*, Wiley, 2002.

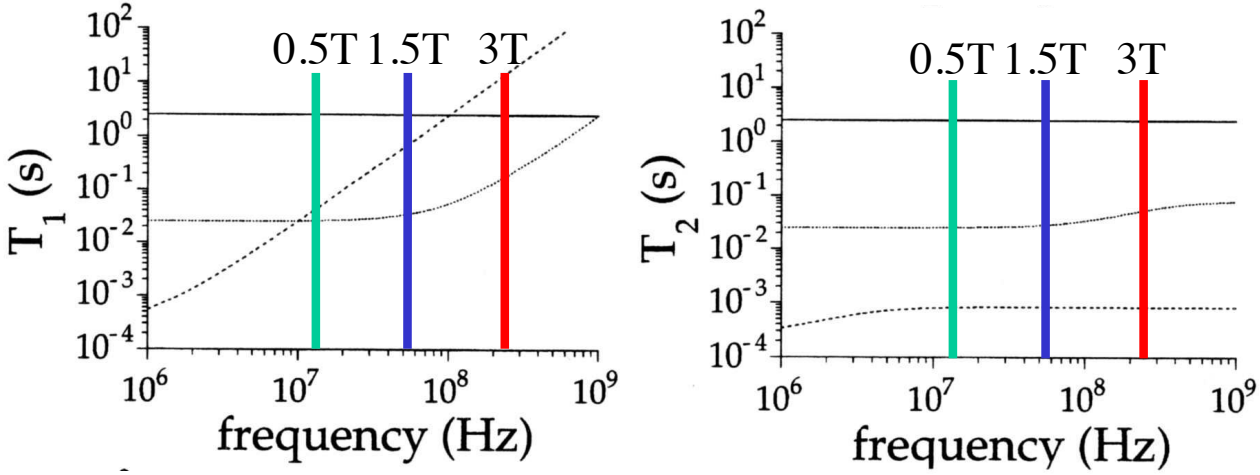

Magic Angle Effects

- Observation: on moderate to short TE sequences, signal intensity of tendons, ligaments, and cartilage depends on tissue orientation with respect to the large B_0 field.

- These highly ordered tissues contain collagen fibers with bound water that is not free to tumble isotropically.

- Dipole interaction among bound water protons is angle dependent.

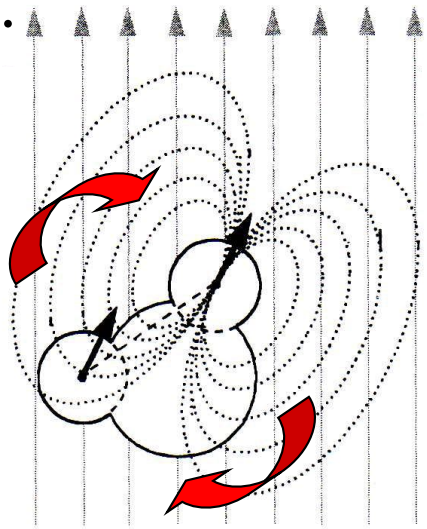

Collagen fiber during hydration

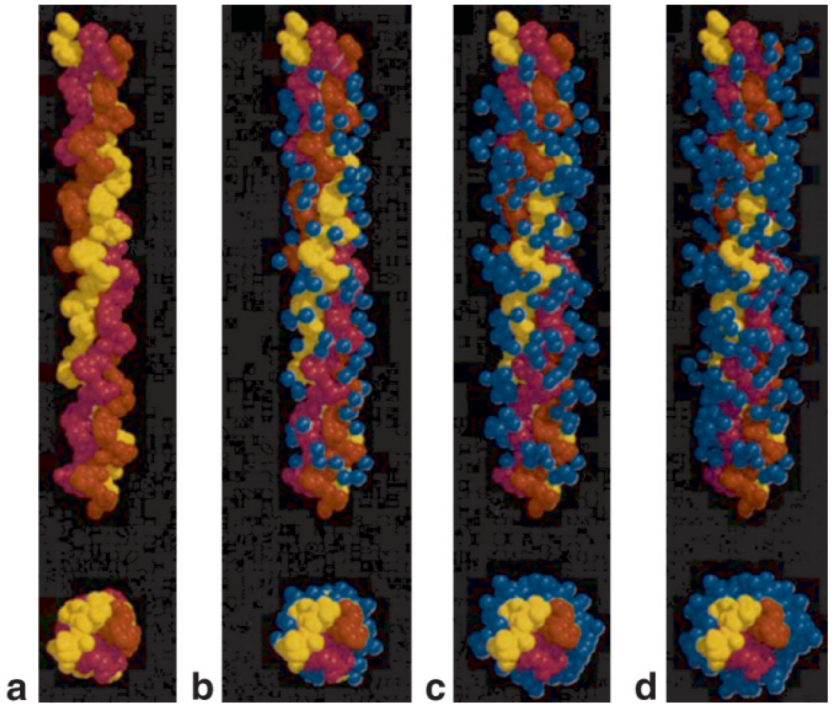

Fullerton , et al. JMRI, 25:345–361 (2007)

The Nuclear Dipolar Coupling Hamiltonian

- Hamiltonian

$$\hat{H}_{dipole} = -\frac{\mu_0 \gamma_I \gamma_S}{2\pi r^3}\hbar\left(\hat{\vec{I}}\cdot\hat{\vec{S}} - \frac{3}{r^2}(\hat{\vec{I}}\cdot\vec{r})(\hat{\vec{S}}\cdot\vec{r})\right)$$ where $\vec{r}$ vector from spin *I* to spin *S*

- Secular approximation:

$$\hat{H}_{dipole} = d\left(3\hat{I}_z\hat{S}_z - \hat{\vec{I}}\cdot\hat{\vec{S}}\right) \quad \text{where} \quad d = -\frac{\mu_0 \gamma_I \gamma_S}{4\pi r^3}\hbar\left(3\cos^2\Theta_{IS} - 1\right)$$

d: dipole coupling constant

Θ_{IS}: angle between B_0 and vector from spins I and S

  - With isotropic tumbling, the time average of $\hat{H}_{dipole} = 0$
  - With non-isotropic tumbling, $\hat{H}_{dipole}(t) \neq 0$

Magic Angle Spinning

- A common technique used in solid-state NMR is to artificially spin the sample in order to average-out dipolar coupling effects.
- Residual dipolar coupling effects disappear is the sample is spun at an angle of $3\cos^2\theta_0 - 1 = 0$ ($\theta_0 = 54.7^\circ$) relative to B_0

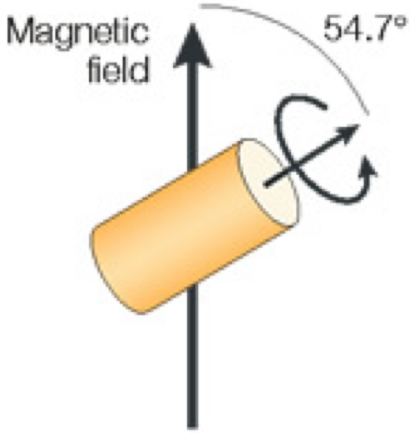

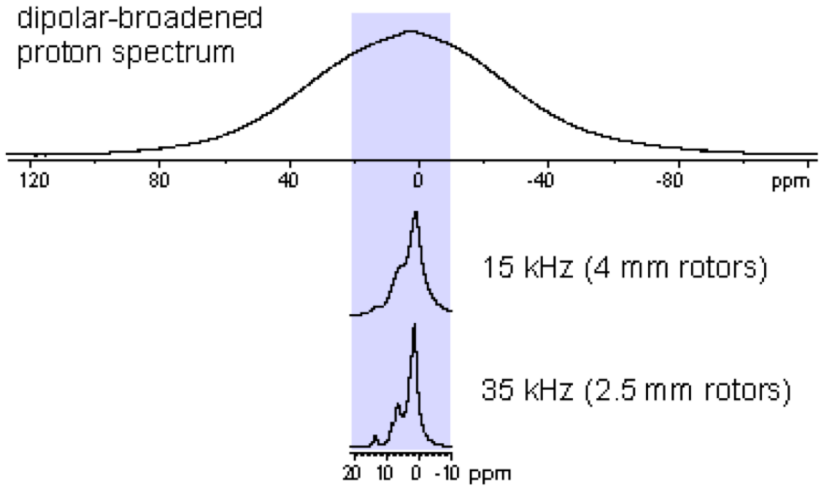

- Magic angle spinning is also use to analyze tissue biopsy samples.

^{1}H MRS of Rat liver biopsy

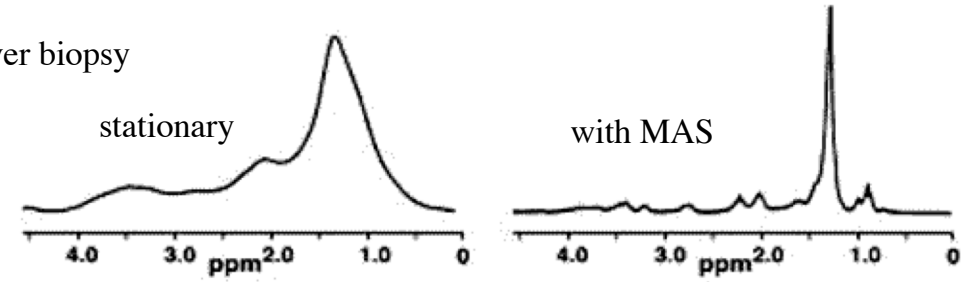

Collagen-bound water

- No spinning allowed for in vivo studies, but we do have restricted tumbling.

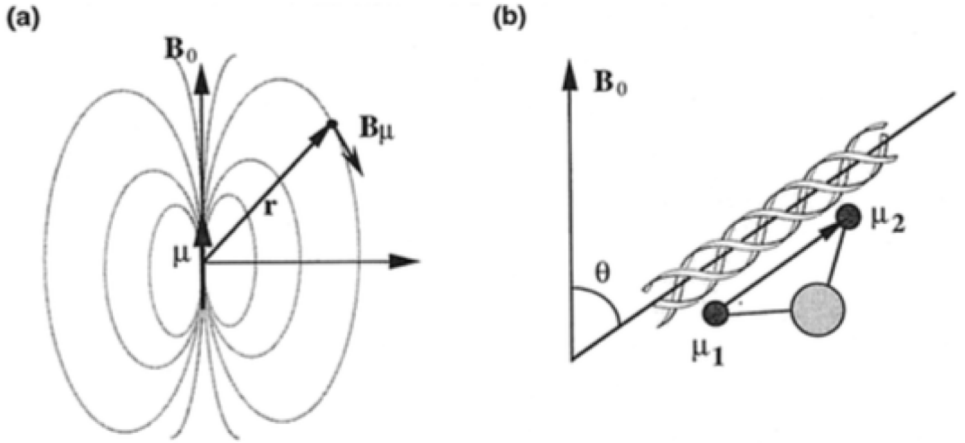

Figure 3. (a) Parameters associated with the magnetic field generated by a classic magnetic dipole $\boldsymbol{\mu}$ at the origin. The *gray lines* represent the local direction of the dipolar field generated by $\boldsymbol{\mu}$. (b) Dipolar interaction between two protons ($\boldsymbol{\mu}_1$ and $\boldsymbol{\mu}_2$) in a water molecule that is bound to a collagen fiber (not to scale). Each proton dipole generates a local dipolar field as shown in (a). Each proton experiences a small contribution of magnetic field from its (many) neighbor protons.

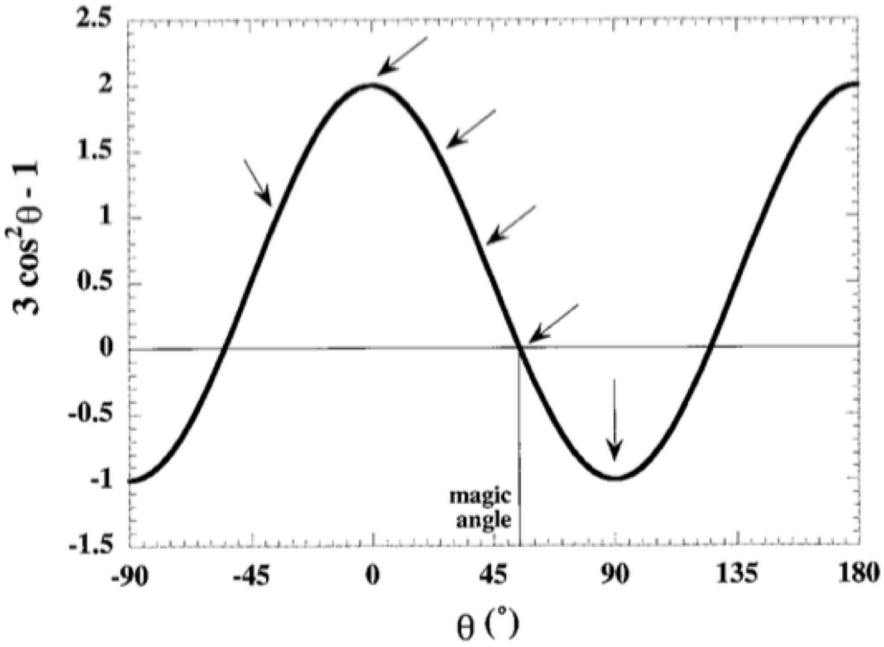

Figure 4. The $(3\cos^2\theta - 1)$ factor in the equation for nuclear dipolar interaction. (The *arrows* identify the discrete sampling points used in the microscopic MRI experiments described in text.[40]) (Reprinted from Xia Y. Relaxation anisotropy in cartilage by NMR microscopy (μMRI) at 14 μm resolution. Magn Reson Med, Copyright © 1998, John Wiley & Sons, Inc. Reprinted by permission of Wiley-Liss, a subsidiary of John Wiley & Sons, Inc.)

Xia, et al. Investigative Radiology, Volume 35, Number 10, 602–621 (2000)

Example: Tendon Imaging

- T_2 of tendons is strongly dependent on the angular orientation with respect to B_0: magic angle = 54.7°

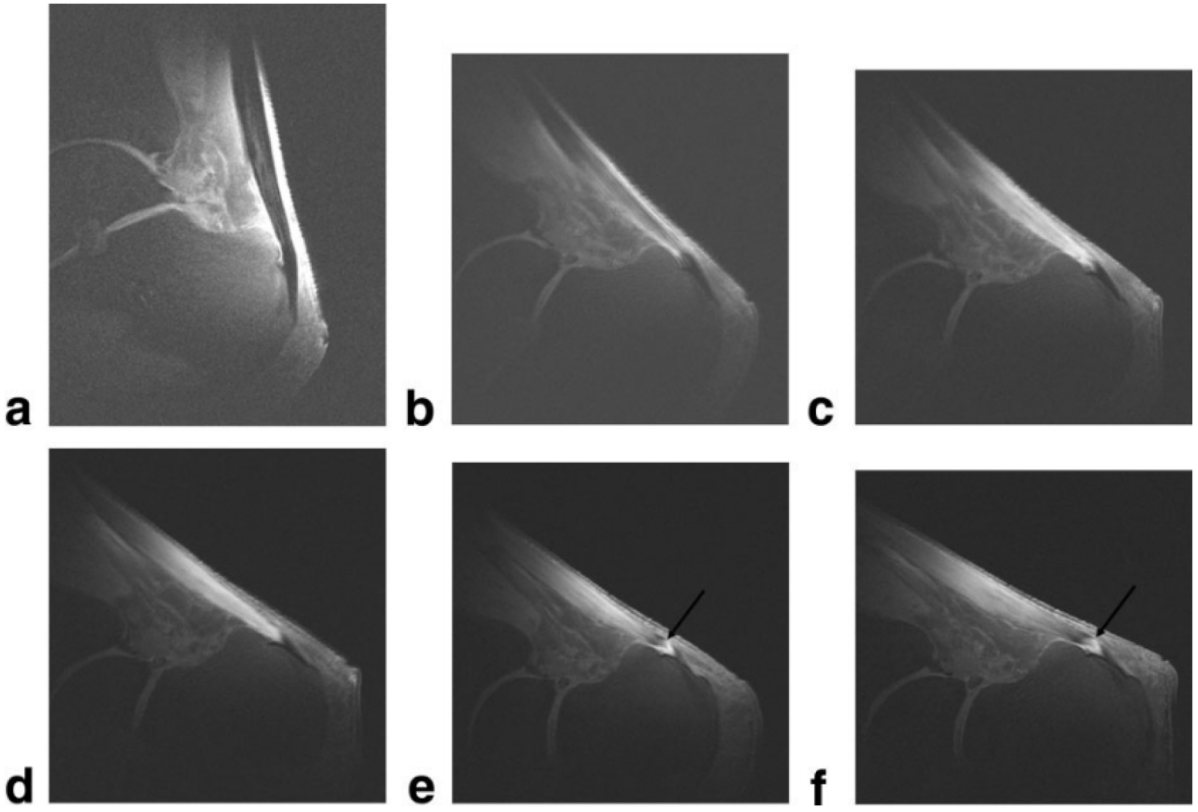

Bydder , et al. JMRI, 25:290–300 (2007)

Figure 2. Achilles tendon at 10° (**a**), 30° (**b**), 40° (**c**), 50° (**d**), and 60° (**e**) to B_0. The signal intensity increases with angle in the midtendon region. Contrast is developed around the sesamoid fibrocartilage (arrow).

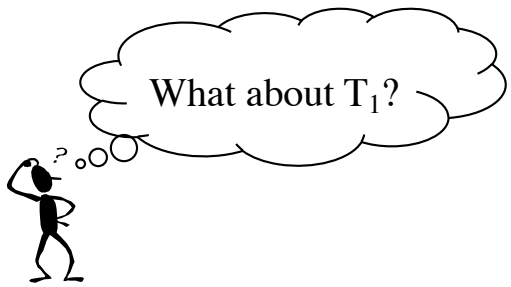

Cross Relaxation in Vivo

Consider the following general pulse sequence:

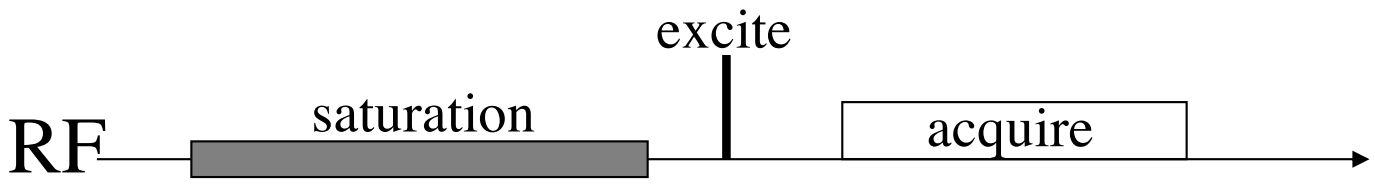

- If no interactions between saturated and observed components, we get familiar results.
  - e.g. fat suppression, water suppression
- What happens if the saturated and observed components interact?

Magnetization Transfer in Tissue

- Two pools of protons

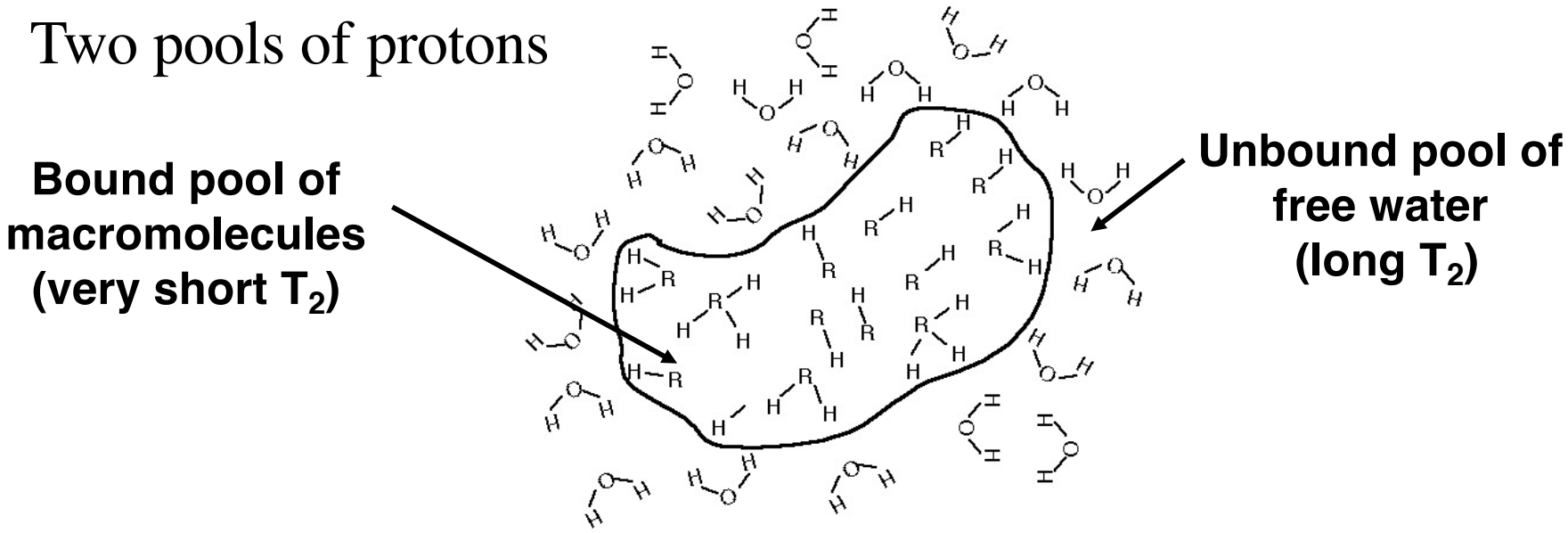

- Selectively saturate short-T_2 pool (bound protons)
- Magnetization exchanged between saturated bound protons and unsaturated mobile protons
- Observe reduced magnetization of longer T_2 (mobile) water protons

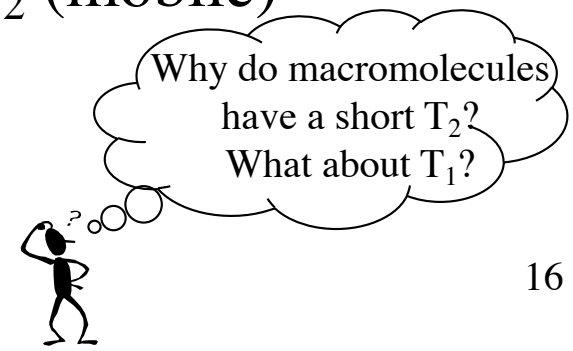

Dipolar coupling leads to NOE effect

$$\mathrm{NOE} = 1 + \frac{\gamma_S}{\gamma_I}\left(\frac{W_2 - W_0}{W_0 + 2W_I + W_2}\right)$$

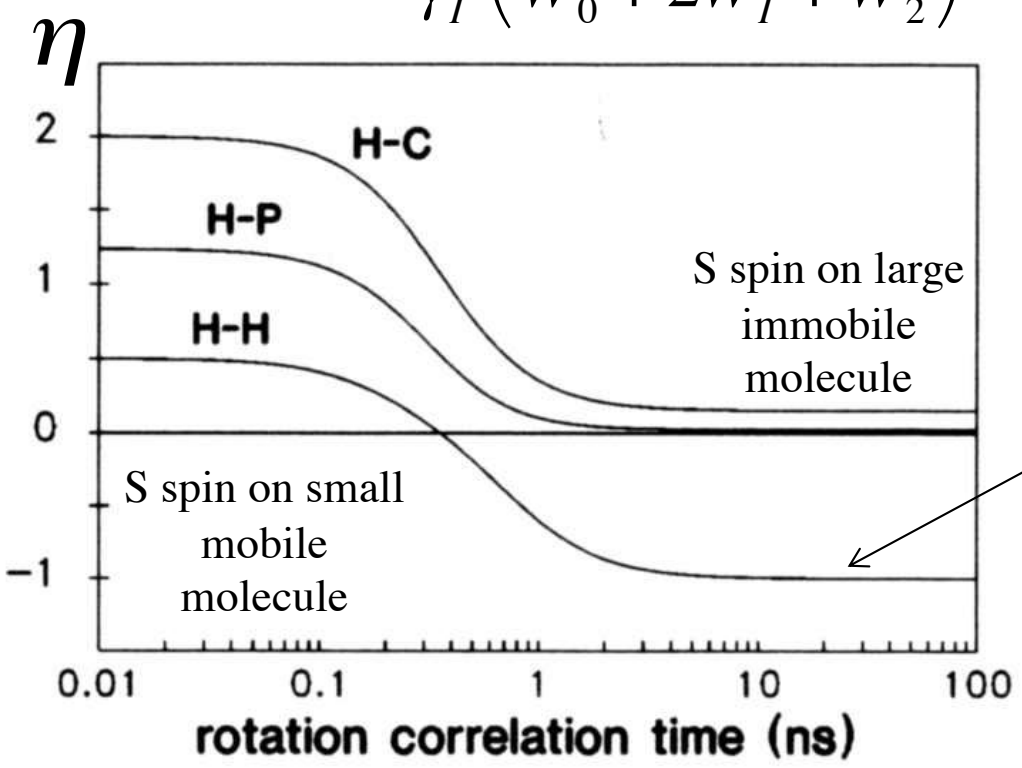

Here we're dealing with slowly tumbling macromolecules. So NOE is negative.

Magnetization Transfer Contrast (MTC)

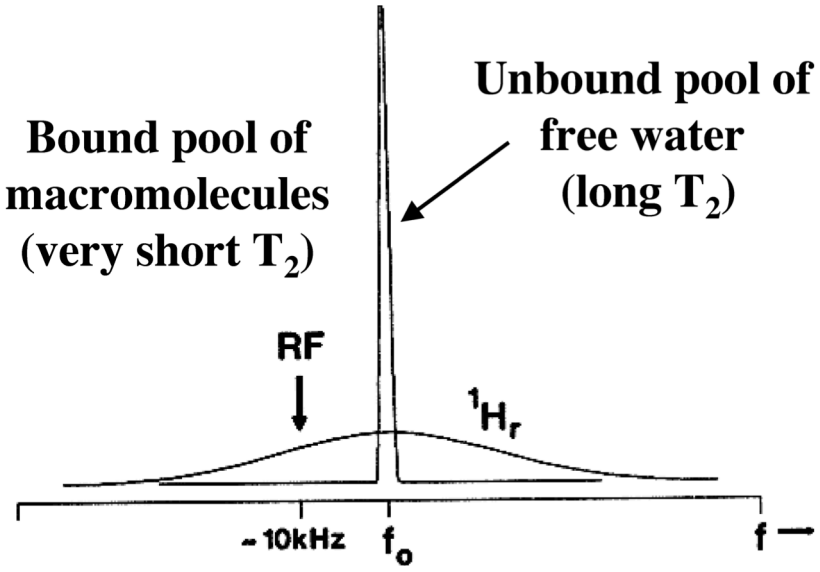

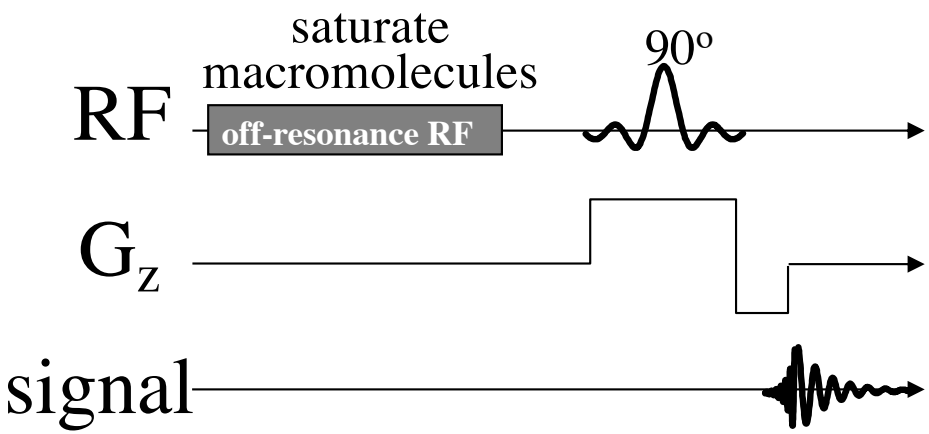

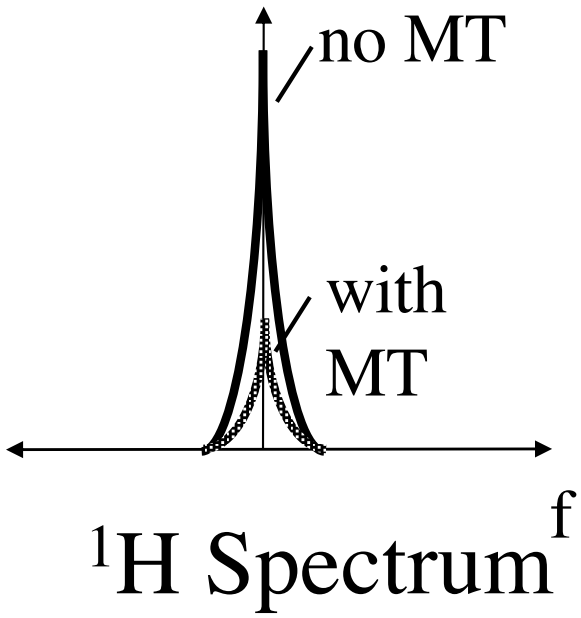

MTC Imaging

- White matter: lots of macromolecules (primarily myelin)
- Gray matter: less macromolecules
- Blood: very few macromolecules

Conventional Imaging **MR Angiography**

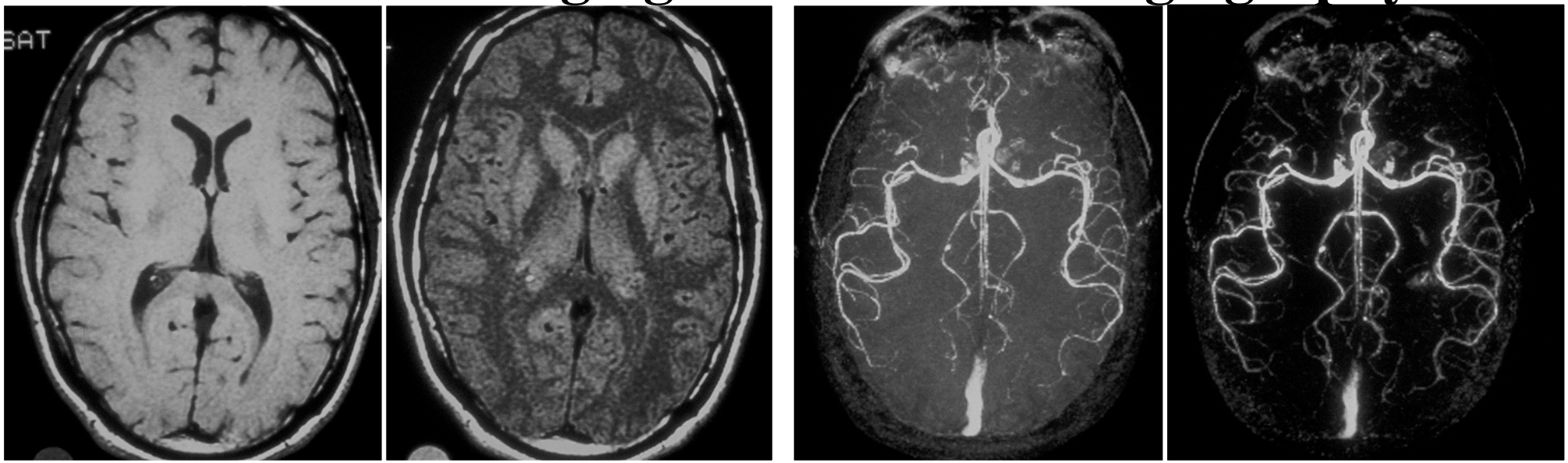

no MTC **with MTC** **no MTC** **with MTC**

MTC MRI

- Interestingly, the equations are very similar if MTC is based on a dipole-dipole interaction (cross relaxation) or a chemical exchange effect.

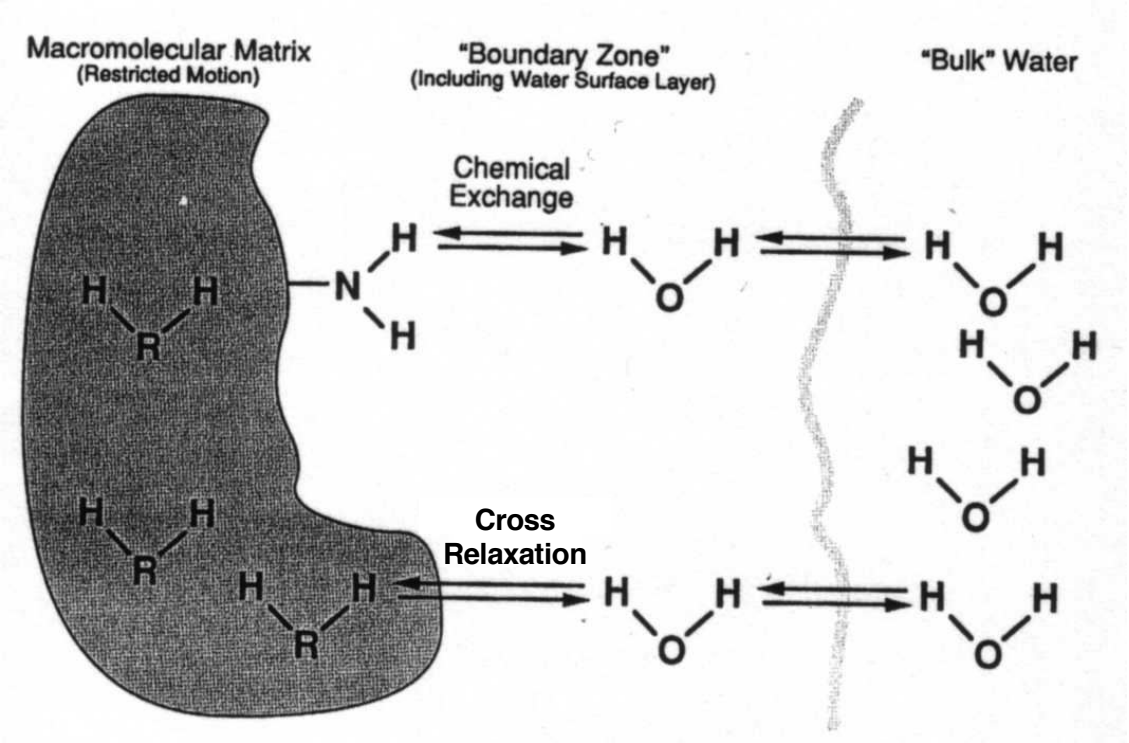

Chemical Exchange Staturation Transfer (CEST)

- Unique image contrast can be generated for spin systems in slow or slow-intermediate chemical exchange.
- The basis idea is to selectively saturate spins in one chemical environment, which are then exchanged into a second environment that can be readily imaged.

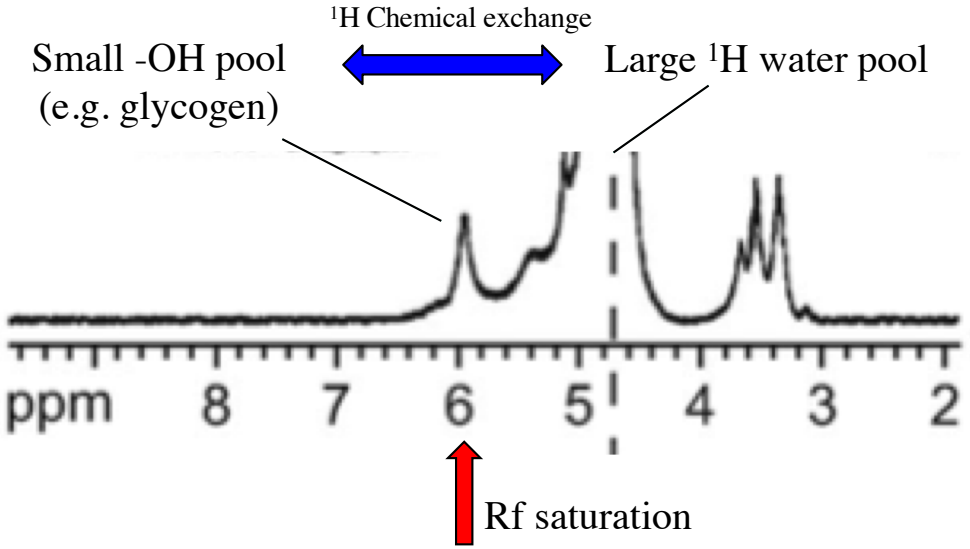

- Image the water with and without Rf saturation
- Need exchange slow enough to have two distinct peaks, but fast enough to allow magnetization transfer before T_1 recovery.

Chemical Exchange Staturation Transfer (CEST)

- Longitudinal magnetization with chemical exchange…

$$A \underset{k_{BA}}{\overset{k_{AB}}{\rightleftharpoons}} B \Rightarrow \begin{aligned} \frac{dM_z^A}{dt} &= \frac{M_z^{A,0} - M_z^A(t)}{T_{1A}} - k_{AB} M_z^A(t) + k_{BA} M_z^B(t) \\ \frac{dM_z^B}{dt} &= \frac{M_z^{B,0} - M_z^B(t)}{T_{1B}} + k_{AB} M_z^B(t) - k_{BA} M_z^A(t) \end{aligned}$$

- Assume slow, slow-intermediate exchange.

- Then, if we can selectively saturate component B with sufficient RF irradiation such that

$$M_z^B = M_z^{B,0} \frac{1 + (\omega_0 - \omega)^2 \left(T_2^B\right)^2}{1 + \omega_1^2 T_2^B T_1^B + (\omega_0 - \omega)^2 \left(T_2^B\right)^2} \approx 0,$$

then the new equilibrium for the A component is $\frac{M_z^A(\infty)}{M_z^{A,0}} = \frac{1}{1 + k_{AB} T_1^A}$

CEST

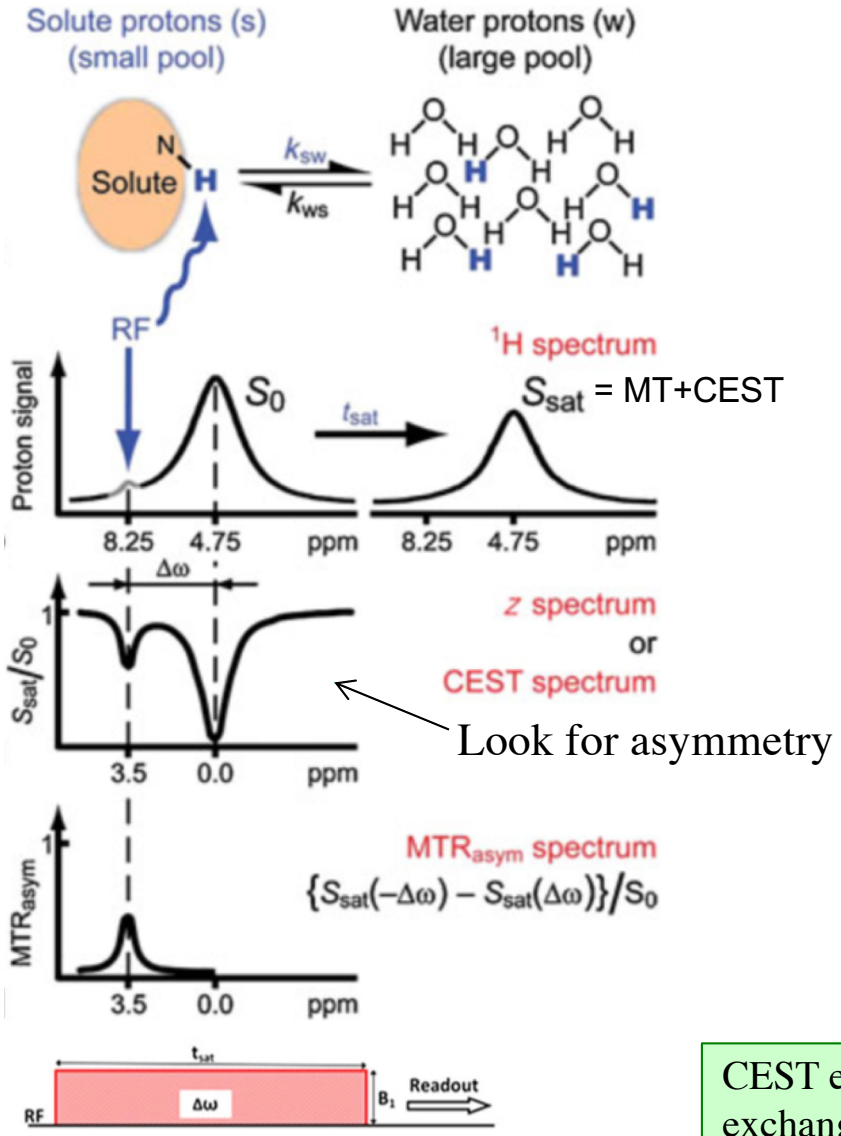

What does the Z-spectrum from the previously described MT effect look like?

Example: 200 mM glycogen

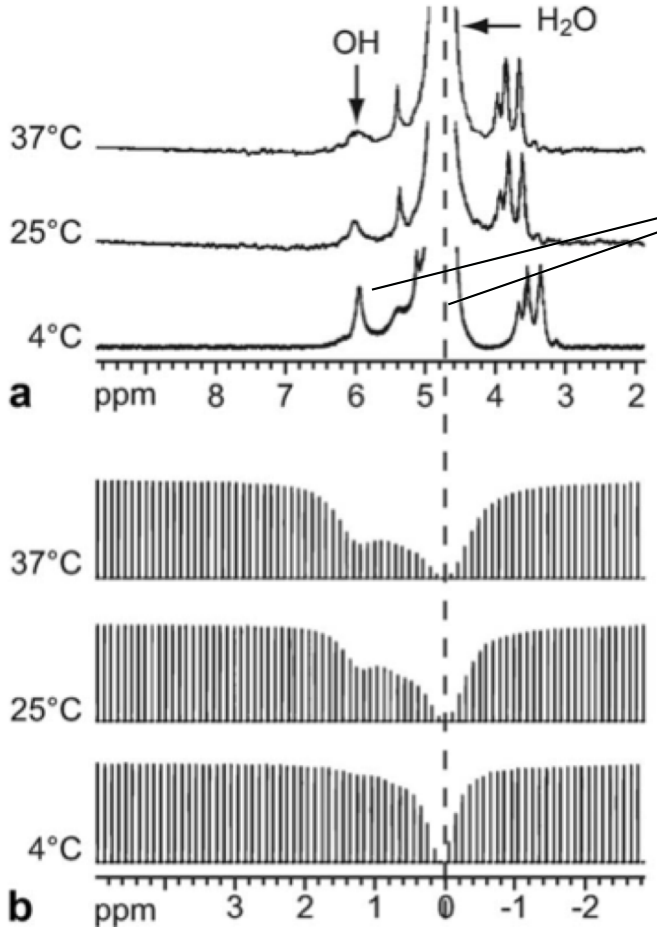

Distinct peaks implies slow exchange,

Why change with temperature?

CEST effect depends on the proton exchange rate, the number of exchangeable protons, the pH of the local environment, T_1, T_2, the saturation efficiency, and the amplitude and duration of saturation pulse.

Van Zijl, et al., MRM 65:927–948 (2011)

Exploitable Exchange Pathways

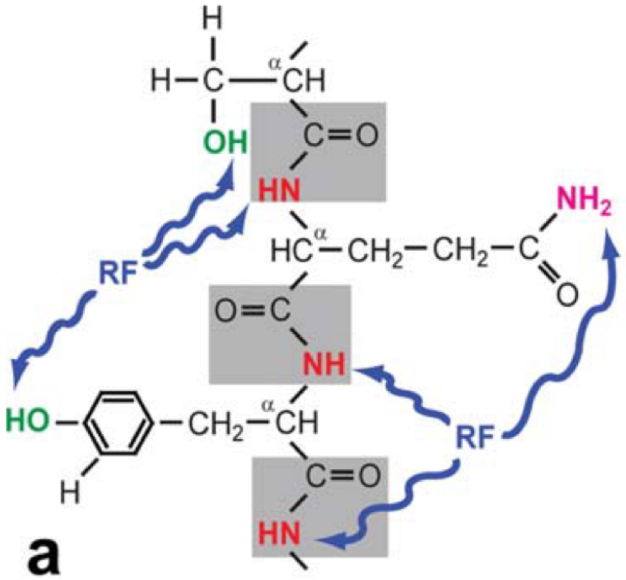

a

ATOM (PROTON) EXCHANGE
small molecules
- diaCEST
- some paraCEST

macromolecular
- supraCEST
- glycoCEST
- gagCEST

multiple molecules
- APT

b

MOLECULAR EXCHANGE
paraCEST
- Ln(III)-OH_2 complexes
- Ln(III)-XH_n complexes
  - *where X represents any coordinated molecule*

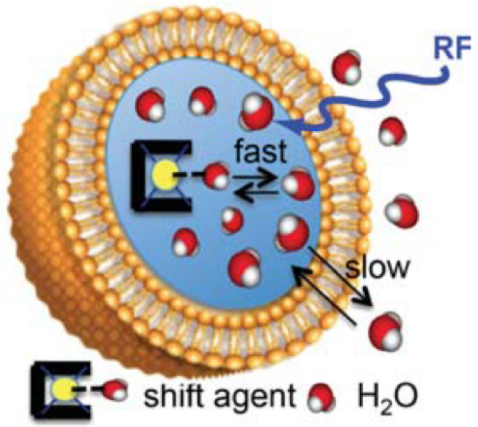

c

COMPARTMENTAL EXCHANGE
lipoCEST

For this lecture, we'll just focus on **a** and leave **b** and **c** for when we discuss contrast agents.

Concentrations needed for ~5% CEST effect with clinical feasible B_1 strengths

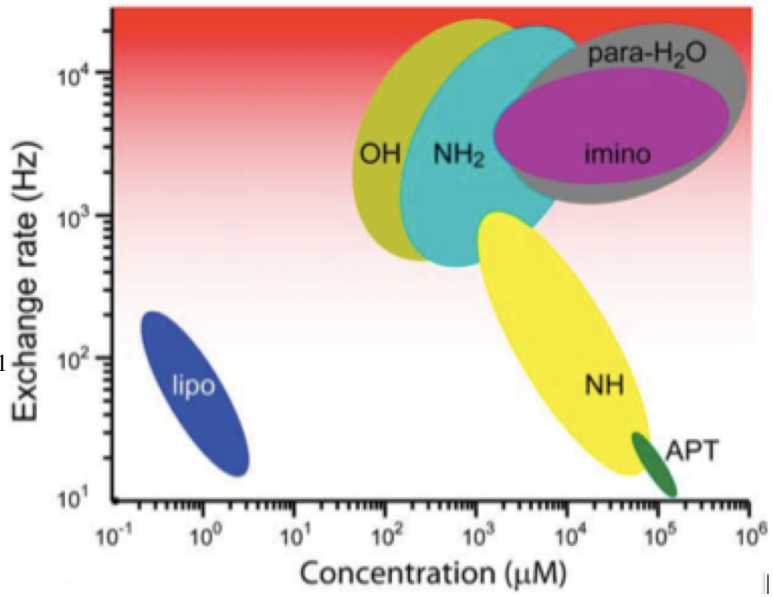

Van Zijl, et al., MRM 65:927–948 (2011)

CEST examples

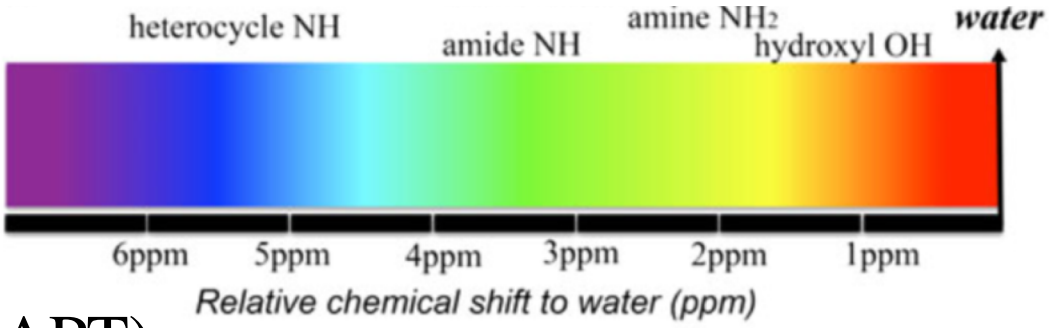

- Amide Proton (-NH) Transfer (APT)
  - Chemical shift ~3.5 ppm below water
  - Very slow exchange rate (~30 s^{-1}) and relatively high concentrations
  - Easy to saturate and hence suitable for 3 T and higher
  - Strong pH dependence on exchange rate
  - Applications: imaging of changes in protein content and pH (e.g tumors)
- Hydroxyl (-OH) CEST
  - Chemical shifts ~1 ppm below water: glucose, glycogen, mI, GAG
  - Moderate exchange rate (~500-1500 s^{-1}) ➔ relatively high-power saturation needed
  - Small $\Delta\omega$ with respect to water ➔ need for high fields (≥7 T), preclinical models
  - Applications: glucose metabolism (glucoCEST, glycoCEST), cartilage (gagCEST)
- Amine (-NH2) CEST (free amino acids, proteins, peptides)
  - Chemical shifts ~3 ppm below water: e.g. glutamate (gluCEST), creatine
  - Faster exchange rate (~2000-6000 s^{-1}) ➔ high transfer efficiency, but high power
  - need for high fields (≥7 T), preclinical models
  - Applications: imaging of protease activity in tumors, pH, glutamate

Some CEST Images

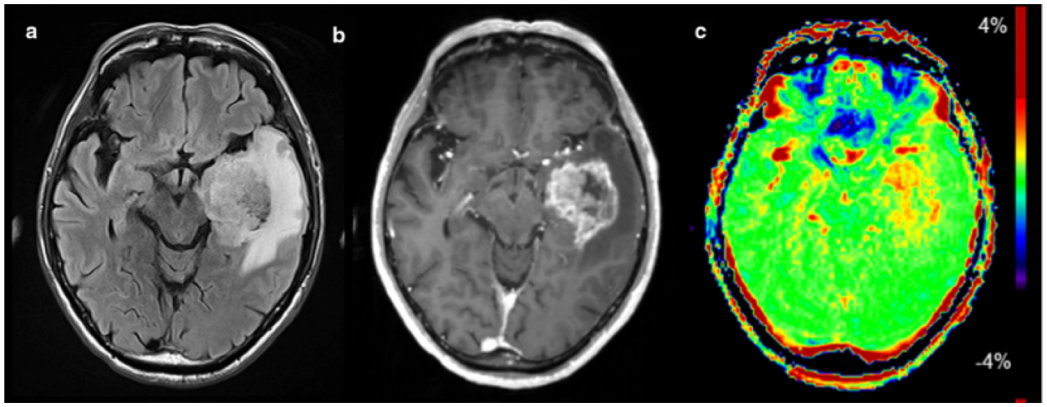

Glioblastoma

Sakata, et al., Journal of Neurooncol, 2015

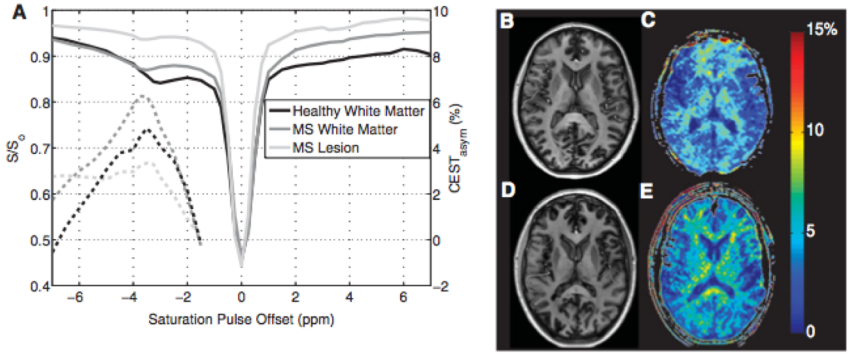

Fig 5. Results of CEST MRI at 7 T on healthy control and MS patient. (A) Z-spectra arising from healthy white matter, MS patient white matter, and MS lesion, solid lines, left *y*-axis. CEST asymmetry is also shown, dashed lines, right *y*-axis. (B) Anatomical image of healthy subject with the calculated APT asymmetry map shown in panel (C). (D) Anatomical image of MS patient with calculated APT asymmetry map found in panel (E).

Multiple Sclerosis

Dula, et al., Journal of Neuroimaging
Vol 23 No 4 October 2013

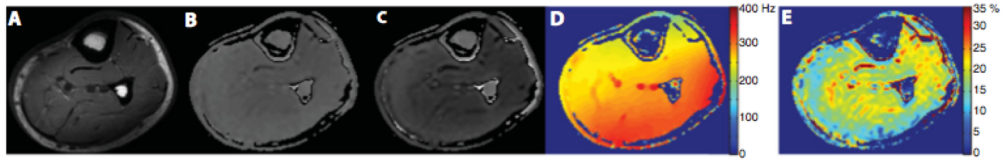

Fig 6. Results from GlycoCEST of skeletal muscle at 7 T. (A) T_1-weighted anatomical image, (B) reference image for glycogen resonance (1.0 ppm), (C) normalized image for glycogen resonance (–1.0 ppm), (D) shift map calculated from polynomial fit with color scale in Hz, and (E) asymmetry map for glycogen (1.0 ppm).

Muscle glycogen

Next Lecture: Redfield theory I